

## Two-phonon character of the lowest electric dipole excitation in $^{142}\text{Nd}$ and in other nuclei near shell closures

M. Wilhelm,<sup>1,2</sup> S. Kasemann,<sup>1</sup> G. Pascovici,<sup>1</sup> E. Radermacher,<sup>1</sup> P. von Brentano,<sup>1</sup> and A. Zilges<sup>1,2,3</sup>

<sup>1</sup>*Institut für Kernphysik, Universität zu Köln, Zùlpicher Strasse 77, D-50937 Köln, Germany*

<sup>2</sup>*Physics Department – WNSL, Yale University, New Haven, Connecticut 06520-8124*

<sup>3</sup>*Institut für Kernphysik, Technische Universität Darmstadt, Schlossgartenstrasse 9, D-64289 Darmstadt, Germany*

(Received 22 April 1997)

A resonant inelastic proton scattering experiment was carried out to investigate the  $\gamma$  decay of the lowest lying  $1^-$  state in the  $N=82$  nucleus  $^{142}\text{Nd}$ . A very high sensitivity for the detection of the  $\gamma$  rays was achieved by combining the Osiris Cube array with a Euroball Cluster detector. The observed  $\gamma$  decay of the dipole excitation is a direct proof of the dominant two-phonon character of the lowest  $1^-$  state in this nucleus. A survey of the branching ratios in the magic neutron number  $N=82$  region and the energy systematics of candidates for two phonon  $1^-$  states in other nuclei in the vicinity of various shell closures point to a high degree of harmonicity of the  $(2^+ \otimes 3^-)$  coupling. [S0556-2813(98)02602-8]

PACS number(s): 21.10.Re, 23.20.Lv, 25.40.Ep, 27.60.+j

### I. INTRODUCTION

The lowest excitations in nuclei near shell closures are usually a  $2^+$  quadrupole oscillation and a  $3^-$  octupole oscillation of the nuclear surface. In the  $N=82$  region these excitations lie at energies of about 1.5 and 2 MeV, respectively. Their typical ground-state transition strengths of  $B(E2, 2_1^+ \rightarrow 0_{g.s.}^+) \approx 15$  Weisskopf units and  $B(E3, 3_1^- \rightarrow 0_{g.s.}^+) \approx 30$  Weisskopf units exhibit the collective structure of these states. If one considers these surface vibrations as ‘‘phonons,’’ an immediate question is whether one can couple two of these phonons to form a multiplet of states with a two-phonon structure. The coupling of two identical phonons, i.e.,  $(2^+ \otimes 2^+)$  and  $(3^- \otimes 3^-)$  has been investigated intensively in recent years, see, e.g., [1–5], and references therein. A pure harmonic coupling of two identical phonons is very unlikely due to the Pauli principle because the same quasiparticle levels can be used to build both phonons. If one considers the coupling of two different phonons this restriction no longer applies.

Candidates for  $2^+ \otimes 3^-$  states have been found in several nuclei [6–13]. The identification was usually based on the energetic position of the states (the energy of a two-phonon state should be the sum energy of the single-phonon constituents) and their relatively strong  $E1$  ground-state transitions of several milli-Weisskopf units (indicating an enhanced electric dipole moment due to an octupole-quadrupole coupling). A recently published work by Heyde and DeCoster [14] showed that the enhanced  $E1$  transition strength of the  $1^-$  state can be explained by taking into account an admixture of  $1p-1h$  excitations at the tail of the giant dipole resonance into the two-phonon state. However, the only direct proof would be the observation of the allowed  $E2$  and  $E3$  transitions to the single-phonon states. In a simple picture one expects that the  $(1_{ph}^- \rightarrow 3_1^-)E2$  transition and the  $(1_{ph}^- \rightarrow 2_1^+)E3$  transition have transition strengths that are identical to those of the  $2_1^+$  and  $3_1^-$  states to the ground state, respectively [15].

Figure 1 shows the estimated ratio between the intensities

of the  $(1_1^- \rightarrow 3_1^-)E2$  and the competing experimentally known  $(1_1^- \rightarrow 0_{g.s.}^+)E1$  ground-state transitions. For this estimate we assumed that the unknown  $B(E2; 1_1^- \rightarrow 3_1^-)$  value is equal to  $B(E2; 2_1^+ \rightarrow 0_{g.s.}^+)$  as predicted in the harmonic coupling scheme. In a previously published measurement [16] the complete  $\gamma$  decay of the first electric-dipole excitation could be observed in  $^{144}\text{Sm}$ . Due to the predicted relative  $\gamma$  intensities (Fig. 1) and in order to obtain detailed systematic information on the two-phonon character of the lowest electric-dipole excitation in this mass region a new investigation on  $^{142}\text{Nd}$  was carried out. One expects a ratio between the intensities of the  $(1_1^- \rightarrow 3_1^-)E2$  transition and the ground-state transition of the  $1_1^-$  state of about 1% for  $^{142}\text{Nd}$ . However, the sensitivity limit of the standard Osiris cube setup at the Cologne Tandem accelerator with six Compton sup-

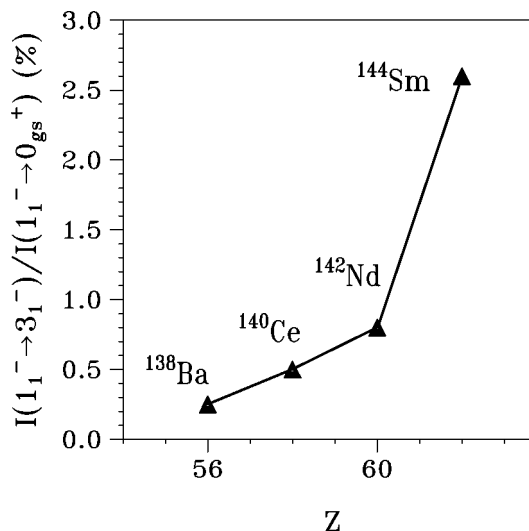


FIG. 1. Expected  $\gamma$  decay intensities of the lowest  $1^-$  state to the octupole vibrational state relative to the intensity of the  $E1$  ground-state transition in even  $N=82$  isotones. Here the unknown  $B(E2; 1_1^- \rightarrow 3_1^-)$  value is assumed to be equal to the experimentally known  $B(E2; 2_1^+ \rightarrow 0_{g.s.}^+)$  in each nucleus.

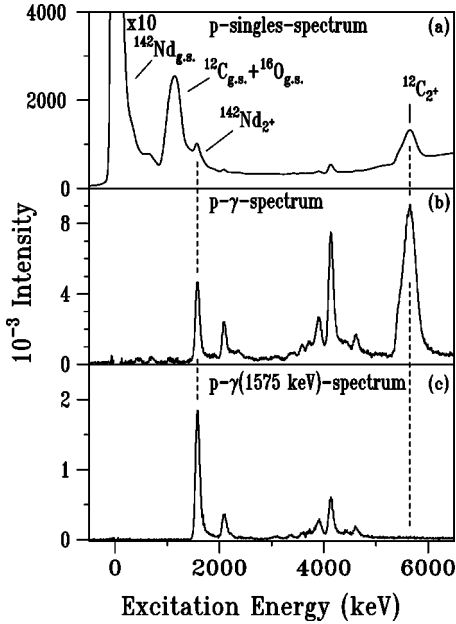


FIG. 2. Proton spectra taken from the  $^{142}\text{Nd}(p, p' \gamma)$  measurement with different coincidence conditions. From the upper to the lower part the proton-singles (a), the proton- $\gamma$  (b), and the proton- $\gamma$  (1575 keV) spectrum (c) can be seen. The latter includes a coincidence window that corresponds to the 1575 keV  $\gamma$  transition. Peaks originating from inelastic scattering on lighter nuclei contaminating the target ( $^{12}\text{C}$ ,  $^{16}\text{O}$ ) are labeled. One can easily see (dashed lines) the improvement with the different type of coincidence conditions.

pressed Ge detectors was already reached with the experiment on  $^{144}\text{Sm}$  which has a more favorable branching ratio. In our previous experiment we could obtain only an upper limit for the  $B(E2)$  decay ratio in  $^{142}\text{Nd}$ . In the new experiment we therefore replaced one of the standard Ge detectors with a Euroball Cluster detector which has a superior detection sensitivity.

It is the aim of this paper to present the results of a resonant ( $p, p' \gamma$ ) study on  $^{142}\text{Nd}$  and to give an overview of the systematic behavior of the  $2^+ \otimes 3^-$  states in the  $N=82$  region and beyond.

## II. EXPERIMENTAL PROCEDURE

We populated the lowest  $1^-$  state with inelastic proton scattering at proton energies corresponding to the isobaric analog resonances (IARs). This excitation mechanism selectively excites high lying negative parity states in even-even nuclei [17]. It therefore overcomes the problem of populating states far above the yrast line with appreciable cross section and allows one to detect weak decay branches. The results of our previous experiment on  $^{144}\text{Sm}$  proved this point [16].

The investigation of  $^{142}\text{Nd}$  was performed at the Tandem Van de Graaff accelerator of the University of Cologne. The incident proton energy was 10.25 MeV, which corresponds to the ( $\nu 3p_{3/2}$ ) IAR. Particle-hole states with negative parity and spin 0 to 4 are thus strongly excited. In addition, the ( $\nu 3p_{3/2}$ ) resonance deexcites to the lowest  $1^-$  state with an appreciable strength [18].

The protons were scattered from a  $1 \text{ mg/cm}^2$  self-supporting metallic  $^{142}\text{Nd}$  foil, enriched to 95.7%. The ex-

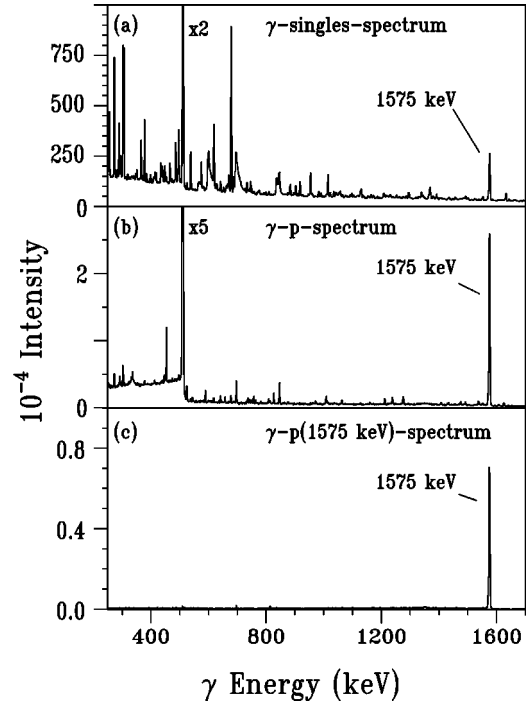


FIG. 3.  $\gamma$  spectra taken from  $^{142}\text{Nd}(p, p' \gamma)$  measurement with different coincidence conditions. From the upper to the lower part the  $\gamma$ -singles (a), the  $\gamma$ -proton (b), and the  $\gamma$ -proton (1575 keV) spectrum (c) can be seen. The latter includes a coincidence window that corresponds to a proton energy loss (i.e., an excitation energy) around 1575 keV. The improvement by the coincidence conditions is very impressive and necessary to observe weak decay branches. As expected, only one  $\gamma$  line occurs in spectrum (c).

periment was carried out at the Osiris-Cube spectrometer [19] which is normally equipped with six escape-suppressed Ge detectors. Two additional Si detectors were used for particle measurement. The detailed setup is discussed in our previous publication [16]. To obtain higher sensitivity for the detection of  $\gamma$  rays one of the six common Ge detectors was replaced by one Euroball Cluster detector. The Euroball project and the development and performance of Cluster detectors are described in detail in Refs. [20–24]. The Cluster

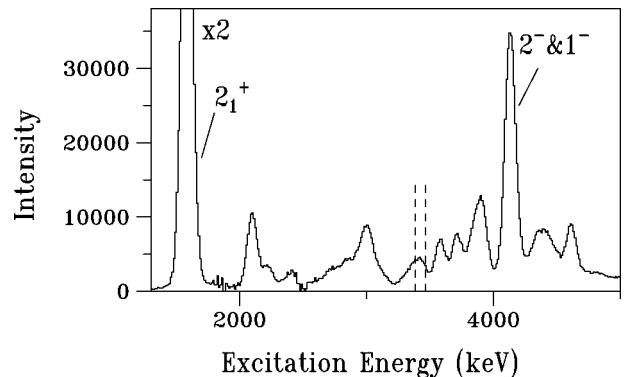


FIG. 4. proton- $\gamma$  coincidence spectrum taken from resonant inelastic proton scattering on  $^{142}\text{Nd}$ . Some strong excitations are labeled with their spin and parity assignment. The label “ $2^-$  &  $1^-$ ” indicates a doublet at 4.1 MeV. The two dashed lines indicate an 80 keV window around the 3424 keV  $1_1^-$  state in  $^{142}\text{Nd}$ . This window was used to sort the  $\gamma$  spectrum shown in Fig. 5.

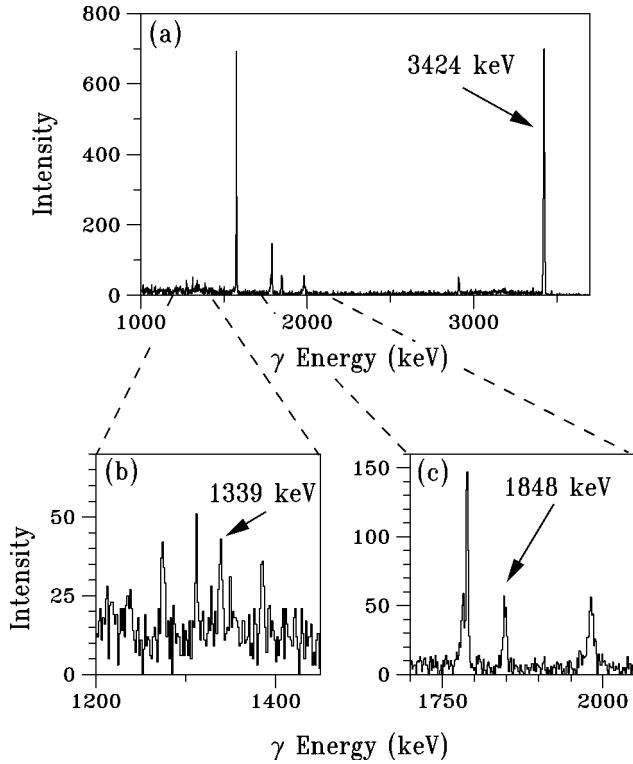


FIG. 5.  $\gamma$  spectra taken from  $^{142}\text{Nd}(p,p'\gamma)$  reaction gated on the coincidence window plotted in Fig. 4 (dashed lines). The upper part (a) presents the  $\gamma$  spectrum from 1.0 up to 3.7 MeV  $\gamma$  energy. In order to identify the interesting  $\gamma$  transitions to the one-phonon states part (a) is expanded [part (b) and part (c)]. One can easily identify the  $\gamma$  lines at 1339 keV (b) and at 1848 keV (c)  $\gamma$  energy. These  $\gamma$  lines could be established as depopulating  $\gamma$  transitions from the  $1_1^-$  state at 3424 keV to the one-phonon states.

detector is the most advanced Ge detector in terms of total absorption efficiency for  $\gamma$  rays and possible coverage of the solid angle with Germanium in a  $4\pi$  spectrometer. The setup used for the experiment on  $^{142}\text{Nd}$  which included one Cluster detector covered a total solid angle of 5.4% of  $4\pi$ . This and the very high efficiency of the detector made the observation of the complete  $\gamma$  decay of the  $1_1^-$  state at 3424 keV in  $^{142}\text{Nd}$  possible. The particle detectors were placed at backward angles with respect to the incoming beam ( $145^\circ$ ) to improve the detection ratio of inelastically to elastically scattered protons. The energy resolution of the measured proton spectra was about 90 keV full width at half maximum. Proton-singles,  $\gamma$ -singles,  $\gamma\gamma$ -, and  $\gamma$ -proton coincidences were recorded with the Cologne data acquisition system [25] during a 120 hour beamtime.

Typical spectra are shown in Fig. 2 and in Fig. 3. From the upper to the lower part Fig. 2 shows proton spectra with different coincidence conditions: proton-singles (a), proton- $\gamma$  coincidence (b), and proton- $\gamma$  coincidence considering only  $\gamma$  rays with energies around the 1575 keV ground-state transition of the first excited state in  $^{142}\text{Nd}$  ( $2_1^+$ ) (c). Both coincidence spectra are time-background corrected to suppress random coincidences. The strong excitation of states with energies between 3.5 and 5.0 MeV (Fig. 2) is evident. This is due to the excitation via the decay of the IAR and results from the selectivity of this excitation mechanism.

In a similar way three  $\gamma$ -ray spectra with different coin-

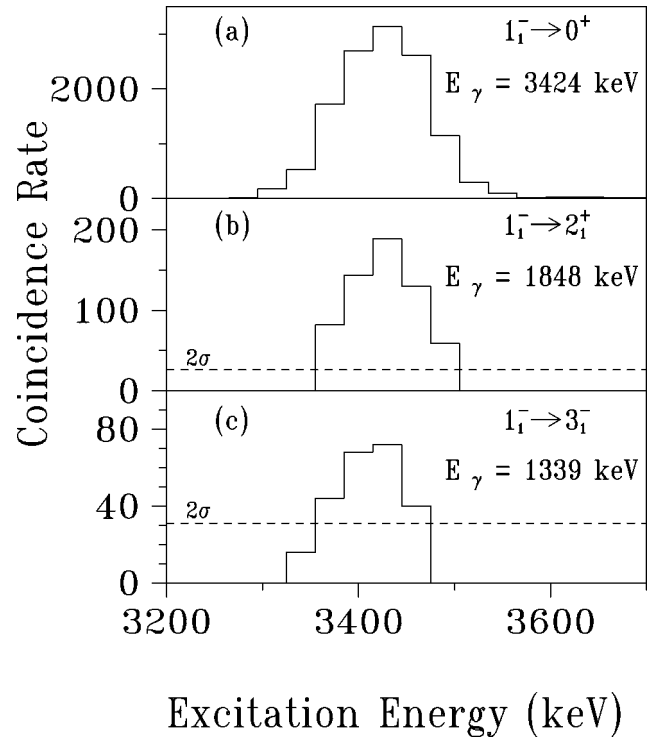


FIG. 6. Coincidence rates of the depopulating  $\gamma$  ray of the  $1_1^-$  state at 3424 keV in  $^{142}\text{Nd}$  plotted versus the excitation energy of the nucleus in the range 3.2 to 3.7 MeV. These rates were extracted from coincidence  $\gamma$  spectra with a window of 30 keV width in excitation energy. The energies of the observed  $\gamma$  transitions of 1848 keV in the middle part (b), of 1339 keV in the lower part (c), and the strong correspondence to the excitation energy at 3424 keV (a) in all plots establish these  $\gamma$  transitions as depopulating transitions of the  $1_1^-$  state. The dashed lines ( $2\sigma$ ) indicate the statistical limit where the intensity of the  $\gamma$  lines could be distinguished from the background intensity.

cidence conditions are presented in Fig. 3. The reduction of the background and the disappearance of numerous  $\gamma$  lines is very impressive. Even more, this technique makes the placement of  $\gamma$  lines in the level scheme possible [Fig. 3(c)]. To establish the observed  $\gamma$  transitions in the level scheme the  $\gamma$ -proton coincidences were evaluated. Coincident  $\gamma$  spectra were analyzed with gates in proton energy corresponding to definite excitation energies. We were thus able to observe very weak  $\gamma$  transitions and to place the corresponding transitions into the level scheme.

### III. THE $\gamma$ DECAY OF THE $1_1^-$ STATE IN $^{142}\text{Nd}$

Figure 4 shows the intensity of the scattered protons which are coincident to any  $\gamma$  ray plotted against the excitation energy of  $^{142}\text{Nd}$ . It is presented in the energy range from 1.4 up to 5 MeV. The strongest excitations are labeled: the first excited state at 1575 keV ( $2_1^+$ ) and the strongly populated particle-hole states at an excitation energy of about 4.1 MeV ( $J^\pi=2^-$  and  $1^-$ ). In addition, the dashed lines indicate the coincidence window around an excitation energy of 3424 keV, the energy of the candidate for the two-phonon  $1_1^-$  state, that was used to extract the  $\gamma$  spectrum presented in Fig. 5. The width of this coincidence window was chosen to be 80 keV which corresponds roughly to the energy reso-

TABLE I. Observed level energies  $E_x$ , initial and final spins  $J_i^\pi$  and  $J_f^\pi$ , transition energies  $E_\gamma$ , decay branching intensities  $I_\gamma$ , and half lives  $T_{1/2}$  of the  $2_1^+$ ,  $3_1^-$ , and  $1_1^-$  states in  $^{142}\text{Nd}$ .

$^{142}\text{Nd}$				
$E_x$ (keV)	$J_i^\pi \rightarrow J_f^\pi$	$E_\gamma$ (keV)	$I_\gamma$	$T_{1/2}$ (fs)
1575.4(2)	$2_1^+ \rightarrow 0_{\text{g.s.}}^+$	1575.4(2)	100.0	$159 \pm 3^a$
2083.5(3)	$3_1^- \rightarrow 2_1^+$	508.1(2)	100.0	$630_{-200}^{+530} a$
3423.9(3)	$1_1^- \rightarrow 0_{\text{g.s.}}^+$	3423.9(2)	100.0	$1.82 \pm 0.37^b$
	$\rightarrow 2_1^+$	1848.2(2)	3.7(3)	
	$\rightarrow 3_1^-$	1339.4(4)	1.0(2)	

<sup>a</sup>Reference [12].

<sup>b</sup>Lifetime deduced from  $\Gamma_0^2/\Gamma = (229 \pm 34)$  meV [9] and the branching ratios determined in this work.

lution obtained in the proton spectrum.

The top part of Fig. 5(a) shows the coincident  $\gamma$  spectrum from 1.0 up to 3.7 MeV  $\gamma$  energy. The strong ground-state transition of the  $1_1^-$  state at 3424 keV excitation energy dominates this  $\gamma$  spectrum. To recognize the expected weak  $\gamma$  transitions to the one-phonon states the  $\gamma$  spectrum in Fig. 5(a) is expanded. This is shown in part (b) and part (c) of Fig. 5. The measured  $\gamma$  energies of 1848 and 1339 keV are exactly the difference between the energies of the  $1^-$  and  $2^+$  or  $1^-$  and  $3^-$  states, respectively. An additional proof that these weak  $\gamma$  transitions are depopulating  $\gamma$  transitions of the  $1_1^-$  state at 3424 keV is presented in Fig. 6. Here the coincidence rates for the  $\gamma$  rays (i.e., how many  $\gamma$  rays are observed in coincidence with a certain energy of the scattered protons) are given versus the excitation energy. From the upper to the lower part of Fig. 6 the coincidence rates for the 3424 keV ground-state transition (a), for the 1848 keV  $\gamma$  line (b), and for the 1339 keV  $\gamma$  line (c) versus the excitation energy of the nucleus are shown. The correspondence to the excitation energy of the  $1_1^-$  state at 3424 keV is striking in all three plots. Due to these coincidence rates and due to observed  $\gamma$  transition energies the  $\gamma$  lines at 1339 and 1848 keV were identified as the  $(1_1^- \rightarrow 3_1^-)E2$   $\gamma$  transition and as

the  $(1_1^- \rightarrow 2_1^+)E1$   $\gamma$  transition, respectively. We considered the  $\gamma$  transition to the  $2_1^+$  as pure  $E1$  transition due to the higher multiplicity of a possible  $E3$  transition. The other  $\gamma$  lines visible in the lower part of Fig. 5 could be established as depopulating  $\gamma$  transitions of states that are close in energy to the excitation energy of about 3424 keV. This is due to the width (80 keV) of the proton coincidence window mentioned above. The 1339 keV  $(1_1^- \rightarrow 3_1^-)E2$   $\gamma$  transition was observed for the first time. The  $\gamma$  decay to the  $2_1^+$  state was already known [12] and its relative intensity could be confirmed in this measurement. The complete  $\gamma$  decay of the lowest electric-dipole excitation at 3424 keV is summarized in Table I. The relative intensities compared to the  $E1$  ground-state transition were determined to be 1.0(2)% for the 1339 keV  $(1_1^- \rightarrow 3_1^-)E2$   $\gamma$  transition and 3.7(3)% for the 1848 keV  $(1_1^- \rightarrow 2_1^+)E1$   $\gamma$  transition. The lifetime of the  $1_1^-$  state was corrected with the new branching ratio. We determined  $T_{1/2} = (1.82 \pm 0.37)$  fs and  $\Gamma = (251 \pm 51)$  meV from the known value  $\Gamma_0^2/\Gamma = (229 \pm 34)$  meV [9].

#### IV. DISCUSSION

The results which are presented in the previous section confirm the proton- $\gamma$  coincidence method as a fruitful tool to observe weak  $\gamma$  transitions. As mentioned above, one expects a strong  $E2$  decay from the two-phonon  $1_{\text{ph}}^-$  state to the  $3_1^-$  state. The simple harmonic phonon picture predicts the strength of this  $E2$  decay to be equal to that of the simple quadrupole-phonon annihilation depopulating the  $2_1^+$  state. Table II shows the experimental  $B(E2)$  value of the  $2_1^+ \rightarrow 0_{\text{g.s.}}^+$  quadrupole-phonon annihilation [12.0(2) W.u.] and the newly determined  $B(E2)$  value of the  $\gamma$  decay of the lowest electric-dipole excitation at 3424 keV to the  $3_1^-$  state. This strength of about 15.7(33) W.u. is within the experimental error the quadrupole-phonon annihilation strength from the  $2_1^+$  state. This experimental agreement is a very strong direct proof of the dominantly two-phonon character of the lowest electric-dipole excitation in  $^{142}\text{Nd}$ .

TABLE II. Reduced transition probabilities (in Weisskopf units) of transitions from the  $2_1^+$ ,  $3_1^-$ , and  $1_1^-$  states in  $^{142}\text{Nd}$ . The values for the  $1_1^-$  state are calculated from Table I. A comparison is made with previous experiments and results obtained from QPM calculations [26]. The deduced  $B(E2; 1_1^- \rightarrow 3_1^-)$  value is proof of the two-phonon structure in the wave function of the  $1_1^-$  state.

$^{142}\text{Nd}$				
$J_i^\pi \rightarrow J_f^\pi$	$E\lambda$	$B(E\lambda) \downarrow$ (W.u.)		
		This work	Experiment Others	Theory Ref. [26]
$2_1^+ \rightarrow 0_{\text{g.s.}}^+$	$E2$		$12.0 \pm 0.2^a$	13.5
$3_1^- \rightarrow 0_{\text{g.s.}}^+$	$E3$		28.6 <sup>a</sup>	27.4
$3_1^- \rightarrow 2_1^+$	$E1$		$(4.3_{-2.0}^{+2.1}) \times 10^{-3} b$	$6.4 \times 10^{-3}$
$1_1^- \rightarrow 0_{\text{g.s.}}^+$	$E1$	$(3.3 \pm 0.7) \times 10^{-3}$	$(3.1_{-0.4}^{+0.6}) \times 10^{-3} b$	$6.2 \times 10^{-3}$
		$(3.1 \pm 0.5) \times 10^{-3} c$		
$1_1^- \rightarrow 2_1^+$	$E1$	$(0.77 \pm 0.16) \times 10^{-3}$	$(0.61_{-0.21}^{+0.29}) \times 10^{-3} b$	$0.11 \times 10^{-3}$
$1_1^- \rightarrow 3_1^-$	$E2$	$15.7 \pm 3.3$		13.7

<sup>a</sup>Reference [28].

<sup>b</sup>Reference [12].

<sup>c</sup>Reference [9].

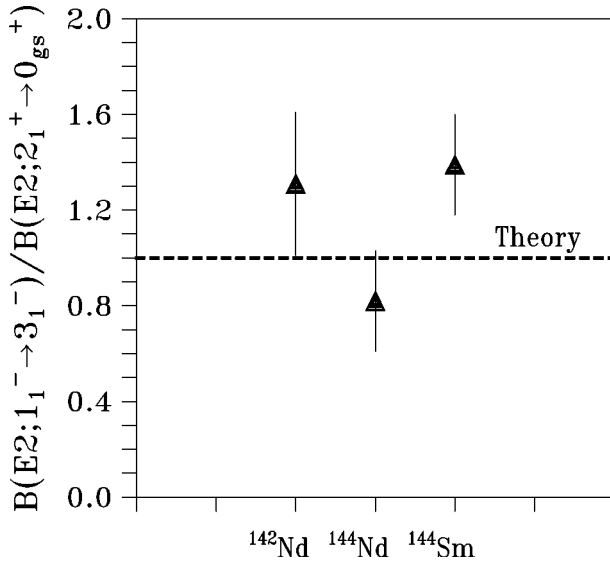


FIG. 7. Experimental  $B(E2; 1_1^- \rightarrow 3_1^-)$  values of the  $A=140$  mass region. The ratio of this value relative to the  $B(E2; 2_1^+ \rightarrow 0_{gs}^+)$  value is plotted for the nuclei  $^{142}\text{Nd}$ ,  $^{144}\text{Nd}$ , and  $^{144}\text{Sm}$ . The simple harmonic phonon picture predicts a ratio of unity for each nucleus. The experimental results agree with this prediction within errors. This agreement is a strong proof for the dominant two-phonon character of the lowest electric-dipole excitation in the  $N=82$  region.

In addition, Table II shows the reduced transition strength calculated in the framework of the quasiparticle phonon model (QPM) [26]. The predicted values agree well with the experimental values determined in this work.

Figure 7 presents the first systematics of the  $B(E2)$  strength of the  $\gamma$  decay of the lowest electric-dipole excitation to the octupole-phonon state ( $3_1^-$ ) in the  $A=140$  mass region. Here the experimental ratio  $B(E2; 1_1^- \rightarrow 3_1^-) / B(E2; 2_1^+ \rightarrow 0_{gs}^+)$  is plotted for each nucleus. The dashed line (theory) indicates the theoretical ratio (1.0) that is expected from the simple harmonic phonon picture. The values presented for the  $N=82$  nuclei could be determined from this work and from our previous publication [16]. The value for  $^{144}\text{Nd}$  ( $N=84$ ) is taken from Ref. [27]. There are no other experimental values available for other nuclei in this mass region. Nevertheless, the systematics shown in Fig. 7 are a

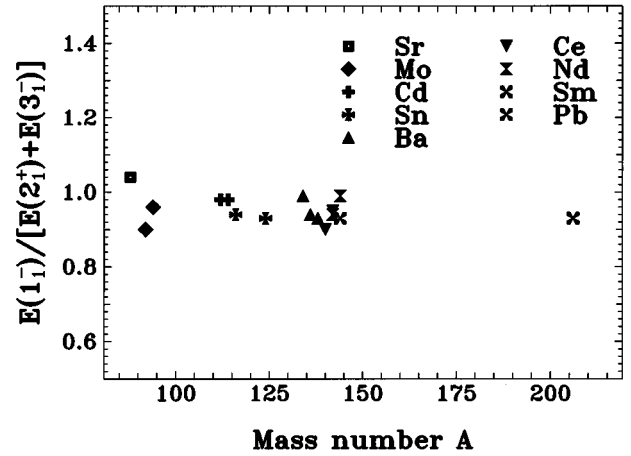


FIG. 8. Systematics of the ratio between the energy of the  $1_1^-$  state and the sum energy of the  $2_1^+$  and  $3_1^-$  state versus the mass number  $A$ . For a pure harmonic coupling without any residual interactions a ratio of 1 is expected.

first strong hint that the existence of very harmonic quadrupole octupole excitations is a general feature of nuclei near closed shells. In Fig. 8 we show the ratio of the energy of the lowest  $1_1^-$  states compared to the sum energy of the  $2_1^+$  and  $3_1^-$  excitations in nuclei ranging from the  $N=50$  nucleus  $^{88}\text{Sr}$  to the  $Z=82$  nucleus  $^{206}\text{Pb}$ . As mentioned above, the energy of the  $1_1^-$  state should be equal to the sum energy for harmonic coupling. One can see that there is a strong correlation and that the energies coincide within 10%. This indicates that the harmonicity of the two phonon quadrupole-octupole excitations seems to be a general phenomenon in nuclei near shell closures. Therefore more experiments investigating the lifetimes and decay patterns of these states are clearly warranted.

#### ACKNOWLEDGMENTS

The authors wish to thank R. F. Casten, A. Gelberg, R.-D. Herzberg, F. Iachello, R. V. Jolos, U. Kneissl, N. Pietralla, H. H. Pitz, and S. W. Yates for many fruitful discussions. This work was supported in part by the DFG under Contract No. Br799/6-2 and by the U.S. DOE under Contract No. DE-FG02-91ER-40609.

[1] A. Bohr and B. Mottelson, *Nuclear Structure* (Benjamin, New York, 1975), Vol. 2, and references therein.  
 [2] A. Aprahamian, D. S. Brenner, R. F. Casten, R. L. Gill, A. Piotrowski, and K. Heyde, *Phys. Lett.* **140B**, 22 (1984).  
 [3] R. F. Casten, *Nuclear Structure from a Simple Perspective* (Oxford University Press, New York, 1990), and references therein.  
 [4] Minfang Yeh, P. E. Garrett, C. A. McGrath, and S. W. Yates, *Phys. Rev. Lett.* **76**, 1208 (1996).  
 [5] J. Enders, P. von Neumann-Cosel, V. Yu. Ponomarev, and A. Richter, *Nucl. Phys.* **A612**, 239 (1997).  
 [6] M. Behar, Z. W. Grabowski, and S. Raman, *Nucl. Phys.* **A219**, 516 (1974).

[7] F. R. Metzger, *Phys. Rev. C* **14**, 543 (1976).  
 [8] R. A. Gatenby, J. R. Vanhoy, E. M. Baum, E. L. Johnson, S. W. Yates, T. Belgya, B. Fazekas, Á. Veres, and G. Molnár, *Phys. Rev. C* **41**, R414 (1990).  
 [9] H. H. Pitz, R. D. Heil, U. Kneissl, S. Lindenstruth, U. Seeemann, R. Stock, C. Wesselborg, A. Zilges, P. von Brentano, S. D. Hoblit, and A. M. Nathan, *Nucl. Phys.* **A509**, 587 (1990).  
 [10] R. A. Gatenby, E. L. Johnson, E. M. Baum, S. W. Yates, D. Wang, J. R. Vanhoy, M. T. McEllistrem, T. Belgya, B. Fazekas, and G. Molnár, *Nucl. Phys.* **A560**, 633 (1993).  
 [11] S. J. Robinson, J. Jolie, H. G. Börner, P. Schillebeeckx, S. Ulbig, and K. P. Lieb, *Phys. Rev. Lett.* **73**, 412 (1994).  
 [12] T. Belgya, R. A. Gatenby, E. M. Baum, E. L. Johnson, D. P.

- DiPrete, S. W. Yates, B. Fazekas, and G. Molnár, *Phys. Rev. C* **52**, R2314 (1995).
- [13] R.-D. Herzberg, I. Bauske, P. von Brentano, Th. Eckert, R. Fischer, W. Geiger, U. Kneissl, H. Maser, N. Pietralla, H. H. Pitz, and A. Zilges, *Nucl. Phys.* **A592**, 211 (1995).
- [14] K. Heyde and C. DeCoster, *Phys. Lett. B* **393**, 7 (1997).
- [15] R. V. Jolos (private communication).
- [16] M. Wilhelm, E. Radermacher, A. Zilges, and P. von Brentano, *Phys. Rev. C* **54**, R449 (1996).
- [17] C. F. Moore, J. G. Kulleck, P. von Brentano, and F. Rickey, *Phys. Rev.* **165**, 1312 (1968).
- [18] L. Bimbot, L. Lessard, S. Santhanam, R. Martin, O. Dietzsch, D. Spalding, K. Schechet, and J. L. Foster, *Phys. Rev. C* **9**, 741 (1974).
- [19] R. Wirowski, M. Schimmer, L. Eßer, S. Albers, K. O. Zell, and P. von Brentano, *Nucl. Phys.* **A586**, 427 (1995).
- [20] J. Eberth, *Prog. Part. Nucl. Phys.* **28**, 495 (1992).
- [21] J. Eberth, H. G. Thomas, P. von Brentano, R. M. Lieder, H. M. Jäger, H. Kämmerling, M. Berst, D. Gutknecht, and R. Henck, *Nucl. Instr. Methods Phys. Res.* **369**, 135 (1996).
- [22] H. G. Thomas, Ph.D. thesis, Institut für Kernphysik, Universität zu Köln, Berlin, 1995.
- [23] R. M. Lieder (unpublished).
- [24] M. Wilhelm, J. Eberth, G. Pascovici, E. Radermacher, H. G. Thomas, P. von Brentano, H. Prade, and R. M. Lieder, *Nucl. Instrum. Methods Phys. Res. A* **381**, 462 (1996).
- [25] M. W. Luig, S. Albers, F. Giesen, N. Nicolay, J. Rest, R. Wirowski, and P. von Brentano, *Verh. Dtsch. Phys. Ges.* **30**, 736 (1995).
- [26] M. Grinberg and Ch. Stoyanov, *Nucl. Phys.* **A573**, 231 (1994).
- [27] J. K. Tuli, *Nucl. Data Sheets* **56**, 607 (1989).
- [28] G. Kinleben and T. W. Elze, *Z. Phys. A* **286**, 415 (1978).